Science of the Total Environment 502 (2015) 224–235

Contents lists available at ScienceDirect

Science of the Total Environment

journal homepage: www.elsevier.com/locate/scitotenv

Identification of dust storm source areas in West Asia using multiple environmental datasets

Hui Cao [a,b,c,*], Farshad Amiraslani [d], Jian Liu [b], Na Zhou [e,c]

[a] Key Laboratory of Ecosystem Network Observation and Modeling, Institute of Geographic Sciences and Natural Resources Research, Chinese Academy of Sciences, Beijing, China
[b] International Ecosystem Management Partnership, United Nations Environment Programme, Beijing, China
[c] University of Chinese Academy of Sciences, Beijing, China
[d] Faculty of Geography, University of Tehran, Tehran, Iran
[e] Xinjiang Institute of Ecology and Geography, Chinese Academy of Sciences, China

HIGHLIGHTS

- We develop a three-step approach for the identification of SDS source areas.
- We map out SDS source areas in Syria, Iraq, Jordan, Iran and Saudi Arabia.
- The SDS source clusters and their main paths in West Asia are identified.

ARTICLE INFO

Article history:
Received 11 July 2014
Received in revised form 28 August 2014
Accepted 9 September 2014
Available online xxxx

Editor: P. Kassomenos

Keywords:
SDS source
HYSPLIT model
MODIS satellite images
Landsat 8

ABSTRACT

Sand and Dust storms are common phenomena in arid and semi-arid areas. West Asia Region, especially Tigris-Euphrates alluvial plain, has been recognized as one of the most important dust source areas in the world. In this paper, a method is applied to extract SDS (Sand and Dust Storms) sources in West Asia region using thematic maps, climate and geography, HYSPLIT model and satellite images. Out of 50 dust storms happened during 2000–2013 and collected in form of MODIS images, 27 events were incorporated as demonstrations of the simulated trajectories by HYSPLIT model. Besides, a dataset of the newly released Landsat images was used as base-map for the interpretation of SDS source regions. As a result, six main clusters were recognized as dust source areas. Of which, 3 clusters situated in Tigris–Euphrates plain were identified as severe SDS sources (including 70% dust storms in this research). Another cluster in Sistan plain is also a potential source area. This approach also confirmed six main paths causing dust storms. These paths are driven by the climate system including Siberian and Polar anticyclones, monsoon from Indian Subcontinent and depression from north of Africa. The identification of SDS source areas and paths will improve our understandings on the mechanisms and impacts of dust storms on socio-economy and environment of the region.

1. Introduction

Sand and dust storms (SDS), which normally happen in arid and semi-arid, could cause areas uninhabitable and bring direct damage to human health (Goudie, 2009) as well as transport and deposition of sediments (Yang et al., 2001). These phenomena usually appear with strong and turbulent wind, blowing over desert or aridisol surface with a reduction of visibility. They could lift large quantities of dust particles into the air and transport them hundreds or thousands of kilometers away (Zoljoodi et al., 2013).

There has been a global concern on sand and dust storms considering their huge impacts on socio-economy, human health and environment. Dust storms could affect transportation industry with the reduction of visibility, cause damages to infrastructures, telecommunications and crops (JAPU, 2013). In addition, through intensifying desertification and drought, reducing water supplies and increasing soil salinity, dust storms will result in greater social-economic losses. Dust storms impact on human health through traffic accidents, respiratory complaints and other diseases (Small et al., 2001). For example, dust could carry many allergens including 107 types of bacteria and 106 fungi types (Almasi et al., 2014). The impact of dust storms on environment is also apparent. Dust transport and deposition could affect air temperatures through absorption and scattering of solar radiation, forming clouds and convectional activities (Wong and Dessler, 2005) and affect geochemical conditions of dust storms areas (Menéndez et al., 2007). In recent

* Corresponding author at: Institute of Geographic Sciences and Natural Resources Research, Chinese Academy of Sciences, Beijing 100101, China.
E-mail addresses: hui.cao@unep-iemp.org (H. Cao), amiraslani@ut.ac.ir (F. Amiraslani).

http://dx.doi.org/10.1016/j.scitotenv.2014.09.025
0048-9697/

years, the role of dust storms in global system, such as sulfur dioxide levels, carbon dioxide levels, marine primary productivity, climate change and biogeochemical cycles, has become increasingly significant (Goudie, 2009).

Combating sand and dust storms needs multi-aspect approaches composed of politics, ecosystem management, economics and capacity-building. Before that, the regional identification of major SDS sources will enable us to focus on the critical regions and to characterize unique features in response to environmental conditions (Esmaili et al., 2006a). With such knowledge we will be able to understand the mechanism of dust generation and transportation, to assess the impacts of socio-economic and environmental consequences, and to find effective strategies in controlling and combating sand and dust storms. Many research methodologies are applied to identify the SDS source areas. Ground-based point measurements were used in the past, especially in the examining of aerosol-related climate issues, although their limitations in providing materials for studying large spatial scales are obvious (Esmaili et al., 2006b). With the development of satellite technology, remote sensing methods have gradually played an important role in identification of SDS source areas (Ekhtesasi and Gohari, 2013; Tsolmon et al., 2008). Using TOMS (Total Ozone Mapping Spectrometer) data, the general source areas of sand and dust storms in the global scope were mapped out (Prospero, 2002). Considering the unique characteristics of dust particles in thermal infrared (TIR) band, TIR was also applied for research on SDS hotspots (Mohammad, 2012). Besides remote sensing tools, many aerosol models have been developed to simulate or forecast the trajectory and dispersion of sand and dust storms (Barnum et al., 2004; Ginoux et al., 2001; Ashrafi et al., 2014; Liu et al., 2007; Lu and Shao, 2001; Wang et al., 2011). Among these models, The HYSPLIT (Hybrid Single-Particle Lagrangian Integrated Trajectory) model is a complete system for computing simple trajectories to complex dispersion and deposition simulations using previously gridded meteorological data (Draxler and Hess, 1998). In recent years, researchers prefer to use synthetic analysis combining meteorological data, remote sensing technology, GIS tools or geological information (Al-Jumaily and Ibrahim, 2013; Boloorani et al., 2013; Hamidi et al., 2013; Taheri Shahraiyni et al., 2014; Tsolmon et al., 2008).

West Asia, especially the Tigris–Euphrates alluvial plain, is suffering from severe desertification caused by many reasons including climate and human induced factors, such as global warming, mismanagement of land use, cultivation, overgrazing, marginal plowing and years of warfare (Hamidi et al., 2013; Keramat et al., 2011; UNDP, 2002). This area has been recognized as one of the most important SDS source areas in the world (Furman, 2003; Goudie, 2009). An analysis of the predicted climate change scenarios portrays a harsher situation for the West Asia Region in the coming years. Whether in the form of desertification, deforestation, or wetland destruction or in the form of population growth, food insecurity and water shortage (e.g. For Iran case, see (Amiraslani and Dragovich, 2011)), the countries in the Region are expected to experience environmental and socio-ecological catastrophic events more than ever before. Most of the countries in the Region are now grappling with frequent sand and dust storms as a result of destructive ecological footprints. This recent phenomenon of SDS has forced authorities in some of these countries, notably Iran and Iraq as the immediate sinks of these dusts, to set up specialized tasking groups at national and regional levels to tackle the issue including the identification of sand-source areas. The impacts of an increase in dust storm in Iran, as one of these affected countries studied in this research, are obvious. This phenomenon has forced the Government to declare a state of emergency for sensitive groups (elderly people, patients and children) and to close schools and public organizations in 70% of provinces, in particular western provinces adjacent to the Iraq border, several times over the recent years.

There is an urgent need to identify the SDS source in West Asia, and then to find efficient solutions in combating sand and dust storms accordingly. In this paper, Syria, Iraq, Iran, Jordan and eastern part of Saudi Arabia are focused as pilot countries in West Asia. Some research have provided direct or indirect proofs of SDS source areas in Iraq and eastern part of Syria, mainly located in Tigris–Euphrates plain while for Jordan, Iran and Saudi Arabia, only indirect clues such as vegetation types, bioclimatic zone or land use distribution have been considered for investigation of sand sources. Previous studies have shown evidence in Syria (Geerken and Ilaiwi, 2004; IFAD, 2007; UNDP, 2002) and Iraq (Alonso-Pérez et al., 2013; DRI, 2012; Yang et al., 2001; Zoljoodi et al., 2013); however sand and dust storms are resulted from various factors and thus any investigation necessitates incorporating multiple technologies and information to refine SDS hotspots.

2. Material and methods

2.1. Geographic data features

Thematic maps of West Asia Region, especially Syria and Iraq, were regenerated based on various sources such as scientific articles, project reports, PhD theses, conference proceedings, global or national reports and documents, etc. (Table 1). These thematic maps, extracting direct or indirect clues of SDS sources (dust source areas, SDS clusters, sand dunes, aridisols, dried alluvial fans and psammophytes, etc.), and were produced under unified mapping standards.

Geographic coordinates of the pilot countries were adopted as reference to digitalize the above-mentioned maps using WGS84 coordinate system and Albers Conical Equal Area Projection.

2.2. HYSPLIT model and meteorological data

HYSPLIT model was originally developed using the concept of a threshold friction velocity which depends on surface roughness (Draxler et al., 2001). Surface roughness is correlated with geomorphology or soil properties. The dust emission rate is computed where the local wind velocity exceeds the threshold velocity for the soil characteristics of that emission cell. Backward trajectory method is used to track sand and dust transport and interaction with the surface.

Meteorological station data for the pilot countries (Fig. 1) were downloaded from the website http://gis.ncdc.noaa.gov/map/viewer/#app=clim&cfg=cdo&theme=hourly&layers=1&node=gis in order to identify the dates of sand and dust storms. According to the definition of World Meteorological Organization, dust storms are resultant of weather turbulences which introduce a high dust mass in the atmosphere, and consequently decrease the horizontal visibility to less than 1000 m. A threshold of humidity is also set in case of other weather phenomena like mist although it seldom happens in West Asia Region.

In this paper, we regarded a meteorological station in relation to record dust storms if the visibility was less than 1000 m and the humidity lower than 80% (Fig. 2). In Fig. 2, the red spots represent the frequency of SDS, and larger spots mean more dust storms happening in the station from 2000 to 2013. To some extent, the SDS frequency can provide clues for the distribution of SDS source. Few stations had no recorded data or had limited data. In this case, we excluded the stations with SDS frequency lower than 10 times as they could hardly be used in our methodology. Number of days with SDS was calculated according to the date in which meteorological stations had recorded dust storms each year. As illustrated in Fig. 3, the number of days with SDS in West Asia had fluctuations prior to 2006 and increased significantly afterward. This diagram also manifests the increasing frequency and intensity of SDS events in West Asia, which need to be addressed with the regional cooperation and effort.

2.3. Remote sensing images

Moderate Resolution Imaging Spectroradiometer (MODIS) images provide near global coverage (95%) with high temporal and spectral resolutions (Zhang et al., 2008). This paper applies MODIS L1B data (from

Table 1
Thematic maps collected for the pilot countries.

Name	Source	Type	Country
Major dust source areas in Iraq	(Alonso-Pérez et al., 2013)	Report	Iraq
Major sand dune fields in Iraq	(Yang et al., 2001)	Report	Iraq
Iraq landform	(DRI, 2012)	Project report	Iraq
Zonation of dust sources and areas	(Gerivani et al., 2011)	Journal article	Iraq, Syria
Soils map of Syria	(IFAD, 2007)	Report	Syria
Human-induced soil degradation in Syria	(UNDP, 2002)	Report	Syria
Severity of Eolian sand accumulation	(Geerken and Ilaiwi, 2004)	Journal article	Syria
Dust storm hot spots in Iran	(UNEP, 2013)	Report	Iran
The land use/cover map of Jordan in year 2010	(Al-Bakri et al., 2013)	Journal article	Jordan
Vegetation map in Jordan	(Bsoul and Mazahreh, 2012)	Presentation	Jordan
Landforms of Saudi Arabia	(PME, 2005)	Report	Saudi Arabia
MODIS land cover data	NASA-LAADS Web	Website	Iran, Jordan, Saudi Arabia

LAADS Web, NASA) with a band combination of 1 (red), 4 (green), and 3 (blue) to validate the SDS trajectories simulated by HYSPLIT Model. Besides, MODIS land cover data of MCD12Q1 were used as supplementary for generating thematic maps to address concern on insufficient SDS evidence in Iran, Jordan and Saudi Arabia.

Considering that the results of HYSPLIT simulation are just presented as discrete points, we incorporated Landsat 8 images (more than 200) for the pilot countries to explore areas with same features. Landsat 8 as a significant improvement of Landsat series satellites consists of two sensors: the Operational Land Imager (OLI) and the Thermal Infrared Sensor (TIRS). As the latest Landsat series, Landsat 8 not only receives stronger signals and improves signal-to-noise performance, but also adds new bands such as coastal and aerosol band (Band 1: ultra-blue), cirrus cloud band (Band 9) and adjusts the wavelength of each band which could avoid the atmospheric absorption feature (Li et al., 2013).

2.4. Methodology

In this research, we followed an approach for identifying SDS source areas in three steps: (1) regeneration and overlaying thematic maps; (2) extracting SDS source points using thematic maps and

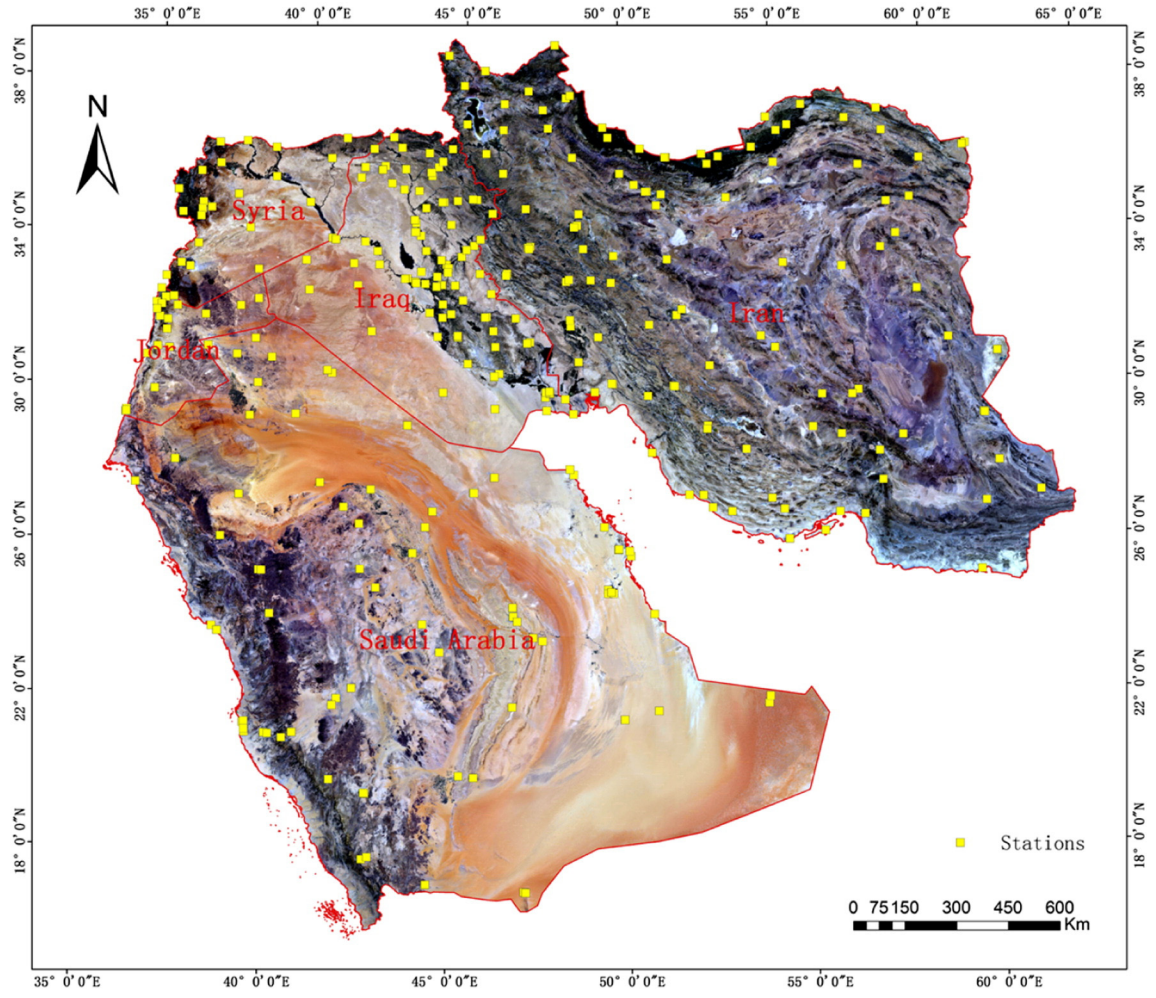

Fig. 1. The distribution of meteorological stations in West Asia.

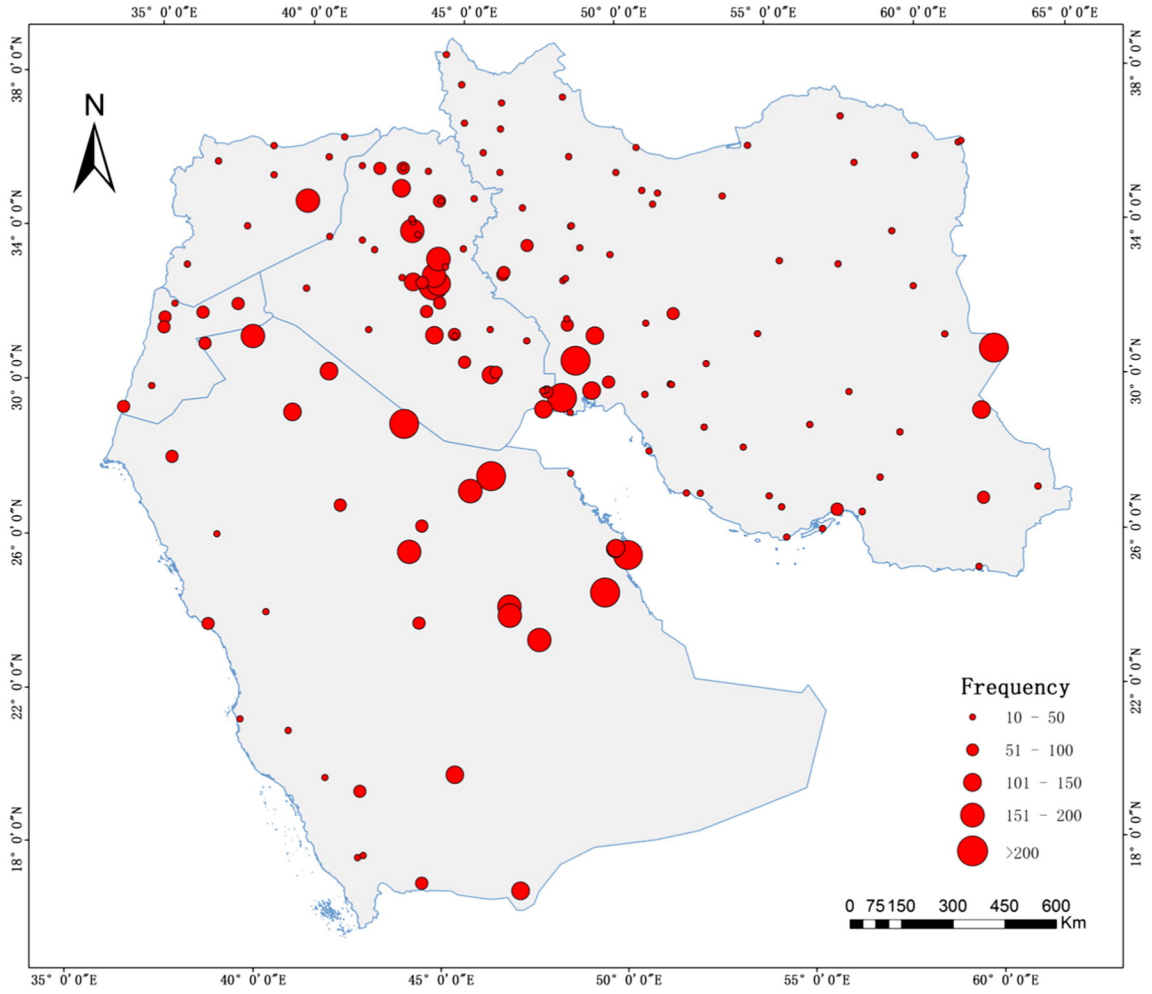

Fig. 2. SDS frequency of the meteorological stations in West Asia Region from 2000 to 2013. (For interpretation of the references to color in this figure legend, the reader is referred to the web version of this article.)

HYSPLIT model; (3) interpretation of SDS source areas on Landsat 8 images.

Firstly, available literature was gathered to gain more insights on sand-generating areas in West Asia Region. As described, thematic maps were regenerated to produce geographic layers using GIS methods. In some cases, websites were searched for gathering new information on some features. For instance, the UNCCD website (http://www.unccd.int/en/Pages/default.aspx) was reviewed to download those National Action Programmes to Combat Desertification of the pilot countries. All efforts were made to generate "potential SDS source" using digital layers (polygons) extracted from thematic maps in Table 1. These digital layers were overlaid to generate new maps to show potential sand-generating source areas. Based on the number of overlapped polygons (areas), the SDS source areas were classified into three classes with low, medium and high potential. A "Low potential SDS source" contains only one layer; a "Medium potential SDS source" area is an overlaying layer composed of two or three layers and a "High potential SDS source" area is a combination of more than three layers. As a result, the potential SDS source map of Iraq and Syria were generated (Fig. 4). Unfortunately, for other countries such as Iran, Jordan or Saudi Arabia, only few thematic layers were available.

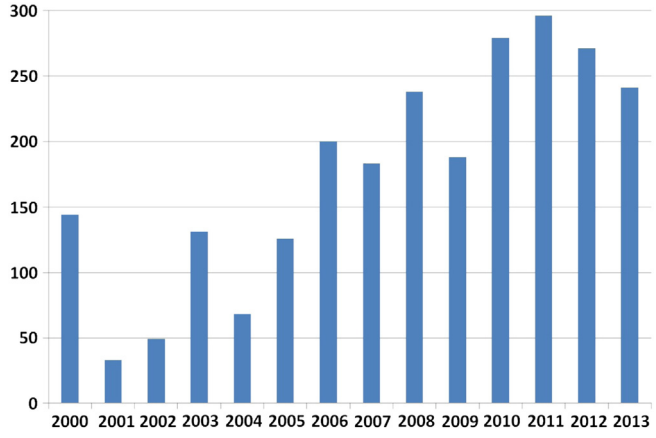

Fig. 3. Number of days with SDS in West Asia Region from 2000 to 2013.

The second step was to simulate the backward trajectories of dust storms using HYSPLIT online model (Draxler and Hess, 1997; Ashrafi et al., 2014). Gridded meteorological data, on one of three conformal (Polar, Lambert, Mercator) map projections, are required to run HYSPLIT model. However, the proper specification of meteorological data is essential for the accuracy of trajectories. In this study, we used GDAS archive (Dec 2004 onward) and NCEP/NCAR Reanalysis (1948 onward) as the input meteorological data. Once the basic meteorological data are processed and interpolated to the internal model grid, trajectories can be computed to test the advection components of the model. The advection of a particle or puff is computed from the average of the three-dimensional velocity vectors for the initial-position $P(t)$ and the first-guess position $P'(t + \Delta t)$. The velocity vectors are linearly

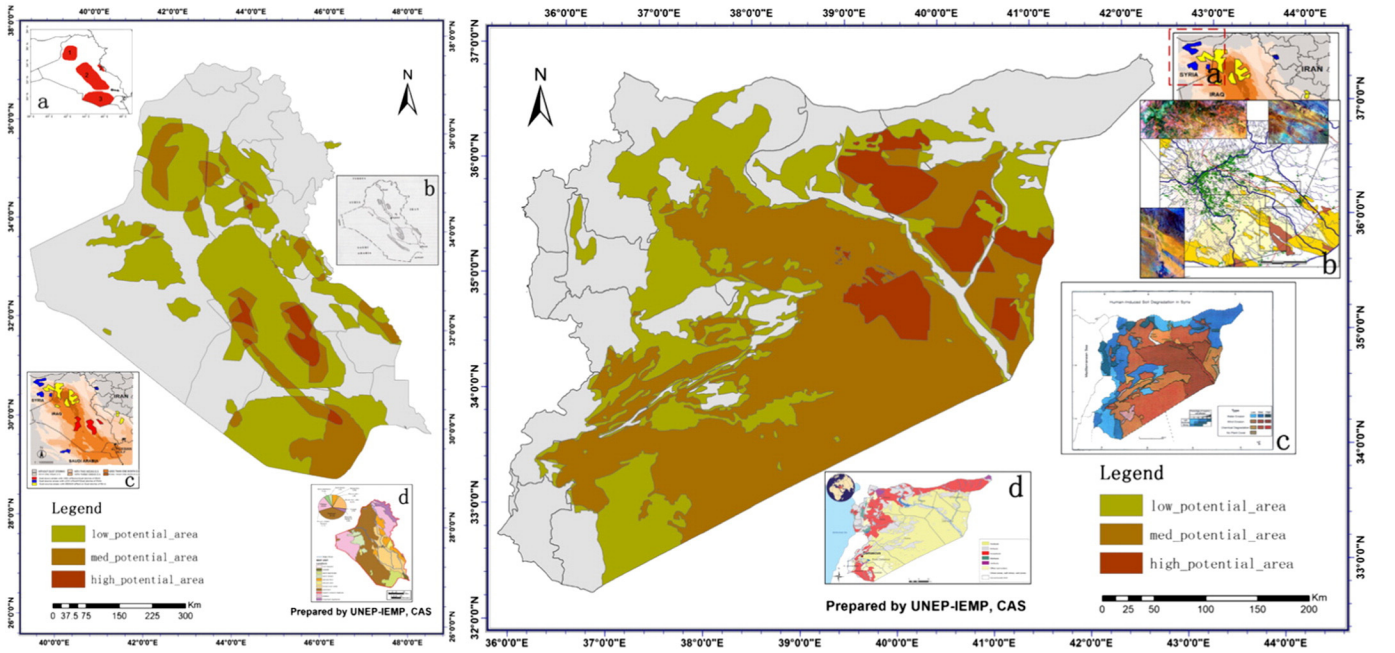

Fig. 4. Potential SDS source distribution of Iraq (left) and Syria (right). Maps were regenerated as digital layers in Iraq include: (a) major dust source areas in Iraq; (b) major sand dune fields in Iraq; (c) zonation of dust sources and areas (Iraq part); and (d) Iraq landform (using sand dunes, sand sheets and alluvial fans). Maps were regenerated as digital layers in Syria include: (a) zonation of dust sources and areas (Syria part); (b) severity of Eolian sand accumulation; (c) human-induced soil degradation in Syria; and (d) soils map of Syria.

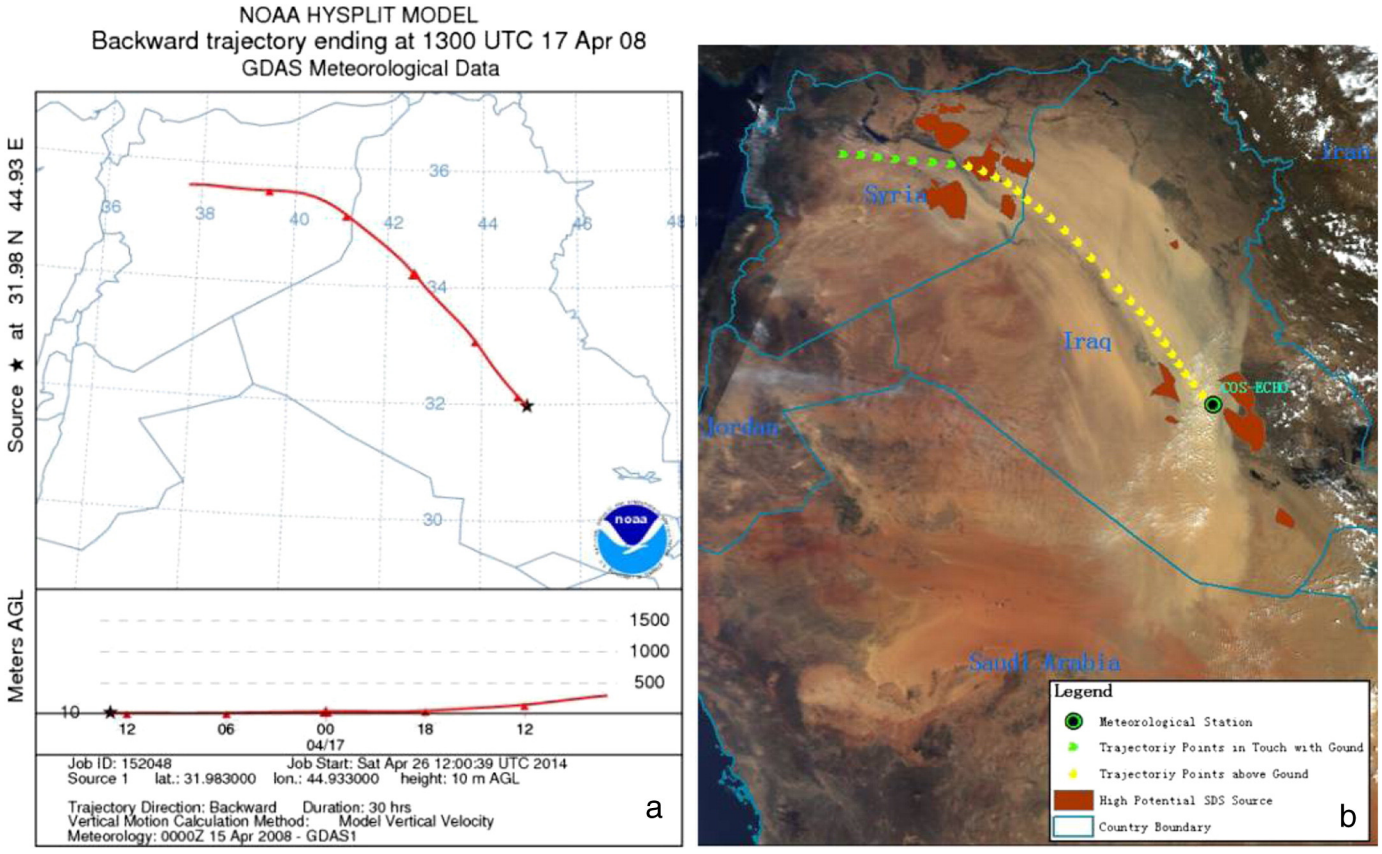

Fig. 5. Dust storm simulation (happened in 17 April 2008) using HYSPLIT online model: (a) GIF format picture; (b) Shapefile trajectory in MODIS images, yellow arrows represent points corresponding with ground. Seeing from (b), the dust storm trajectory is well simulated by HYSPLIT model and the position of first yellow arrow is also consistent with dust storm source shown in MODIS images. In addition, if the arrow is located in "High potential SDS Source" areas, it can be confirmed as SDS source point. (For interpretation of the references to color in this figure legend, the reader is referred to the web version of this article.)

interpolated in both space and time (Draxler and Hess, 1998). The first guess position is

$$P'(t+\Delta t) = P(t) + V(P,t)\Delta t \quad (1)$$

And the final position is

$$P(t+\Delta t) = P(t) + 0.5\left[V(P,t) + V(P',t+\Delta t)\right]\Delta t \quad (2)$$

HYSPLIT backward trajectory online model needs the inputs of starting point and starting height, and generates the outputs of GIS Shapefile trajectories consisting of discrete points with coordinate, time and height. In this study, meteorological stations with records of SDS were used as the starting points with the height of near ground level (10 m). Based on wind speed, particle size and soil size distribution, the wind-blown soil particles were divided into several physical regimes: long-term suspension, short-term suspension, saltation, reptation and creep (Kok et al., 2012). Sand dunes suffered with these different Aeolian modes compose the main SDS source areas in West Asia. In a specific SDS simulation, we regarded the trajectory points as the SDS source areas if they were corresponding to the "High Potential SDS Source" areas (Fig. 5). To ensure the consistency of simulated trajectories with the real situation, more than 50 dust storm events from 2000 to 2013 were collected with MODIS images of which 27 were used to validate the accuracy of backward trajectories. The proportions of dust storms selected in each year are generally coordinated with the number of days with SDS in Fig. 5.

Thirdly, regarding the SDS source spots of Iraq and Syria, we could extract the entire SDS source areas using Landsat 8 images. After different trials, the band composite of 6 (short infrared), 5 (near infrared), and 4 (red) showed better view for the SDS source areas. These areas have distinctive features in different types of purple or ochreous sand dunes accompanied with strips or ripples in the direction of prevailing wind. Considering the difficulty of texture recognition for supervised classification or unsupervised classification, visual interpretation combining geography, climate, SDS paths on MODIS images and knowledge from previous studies were considered as reference to identify SDS source areas (Al-Hurban and Al-Ostad, 2009; Furman, 2003; Hereher, 2009; Li et al., 2013; WMO, 2013). After mapping out SDS source areas in Syria and Iraq, the SDS situation in other three pilot countries were generated using the interpretation experience consequently.

3. Results and discussion

3.1. SDS source distribution

3.1.1. Syria SDS source distribution

Using the methodology mentioned above, the Syria SDS source map was generated (Fig. 6). The main SDS source areas are located in the south-eastern part of Syria with the area of 36,583 km^2. The soil type of SDS source areas in Syria is aridisol represented by gypsids and calcids which equally cover 20% of the country (Ilaiwi, 2001). Gypsids consist of high concentration of gypsum, range from 70% to 95% in extreme cases. They dominate the central and southern parts of Mesopotamia, including the Euphrates and Khabour terraces, the northern part of the Syrian Desert and a large part of the Bichri Mountains. Area 1, located above Euphrates River, is mainly covered by gypsids. As for

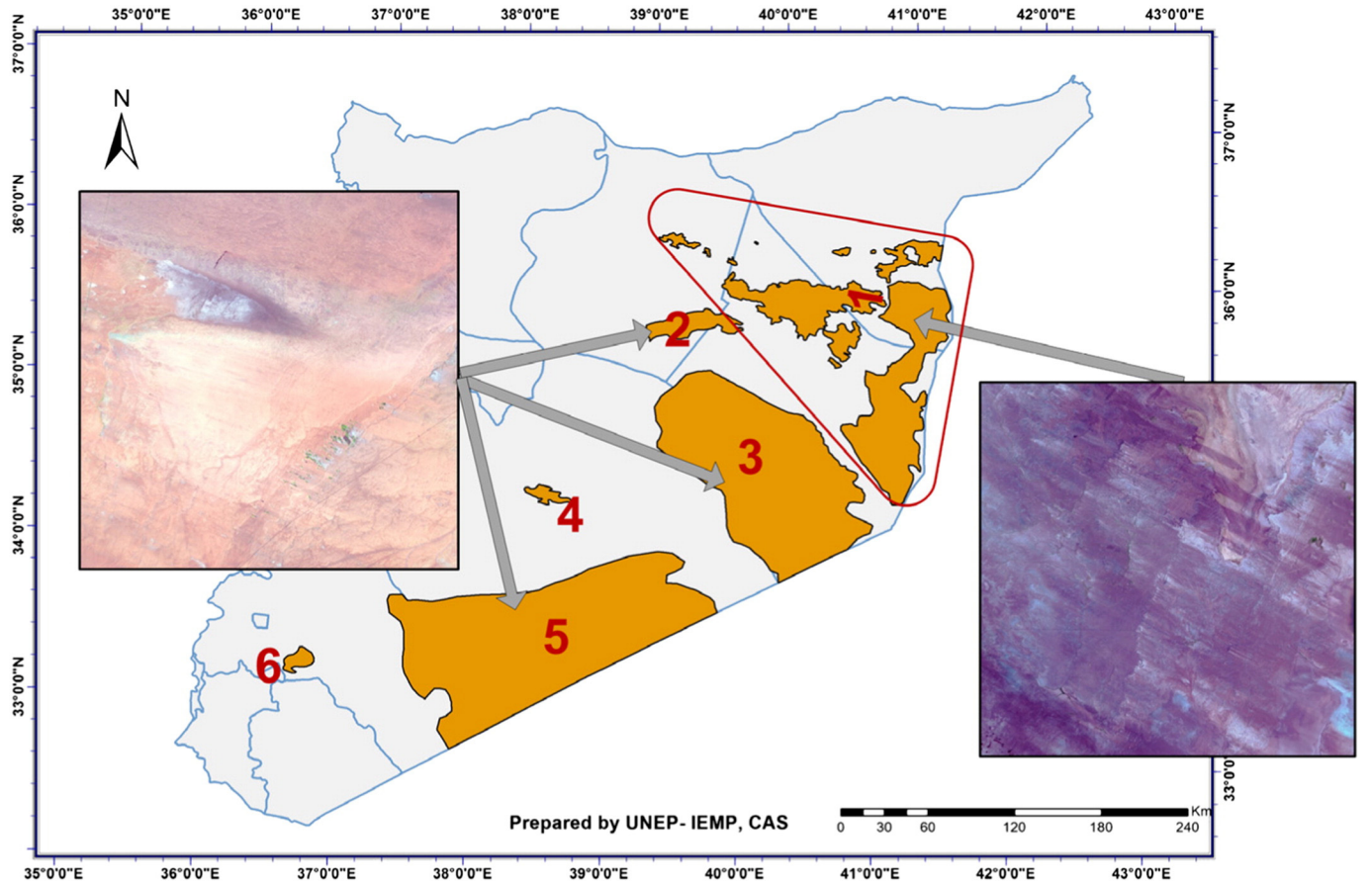

Fig. 6. Syria SDS source area distribution and their characters on Landsat 8 images (6, 5, 4 bands). The right picture shows SDS source features of Area 1, with purple appearance and long sand strips. The left picture mainly presents SDS source features of Areas 2, 3, and 5, which has ochre appearance and continuous sand sheets. (For interpretation of the references to color in this figure legend, the reader is referred to the web version of this article.)

Area 2–6, the soil type generally belongs to Calcids, which are distributed in Syrian part of Hamad plateau and Syrian Desert in southeast and formed by hyper calcic and petrocalcic horizons. Fig. 6 shows the color difference between Area 1 and the others.

Observing the long sand strips, all the SDS source areas suffer from strong wind erosion and the dominating wind direction can be easily identified. In Syria, coastal and northern areas are under control of Mediterranean Sea climate while the southern part suffers Tropical Desert climate. Therefore, Areas 1, 2, 3 suffer from the dominating wind rising from eastern of Mediterranean Sea, or over Cyprus Island, extending deep into southeastern Syria and Iraq. They are major sources of SDS in Syria. Out of 27 dust storms shown by MODIS images, 15 storms result from these three Areas. In these Areas, thick layers of unconsolidated Tertiary sands generate the source material for aeolian sediments (Geerken and Ilaiwi, 2004). Taking Area 2 as an example, intermittent wadis transport sand material originating within unconsolidated Tertiary sands areas during rainy season, and then huge sand sheets will be generated by the prevailing wind from Mediterranean Sea.

Another dominating wind blowing from southwestern of Syria to northeast mainly originates from coastal areas in north of Africa. It makes Areas 4, 5, and 6, which are all parts of Syrian Desert, to be SDS source areas. However, these areas do not show strong or relevant effect to other pilot countries.

3.1.2. Iraq SDS source distribution

The sand and dust storm sources in Iraq can be grouped into 10 areas (Fig. 7) which totally cover about 16% of Iraq. The Iraq SDS sources are mainly distributed in Tigris and Euphrates basin encompassing a large population. Years of desertification and drought resulted by inappropriate farming activities, mistreatment of water resources and climate change contribute to the growth of SDS source areas (JAPU, 2013). Characters of Area 1 show a strong correlation with SDS source in northwest Syria (Fig. 6 Area 1) and this area is regarded as the extension of Syria SDS source. Area 2 and Area 9 possess similar surface features observed through Landsat images. Area 9 has been covered by sand dunes all the time, while Area 2 is degenerated from river valley (DRI, 2012). Large

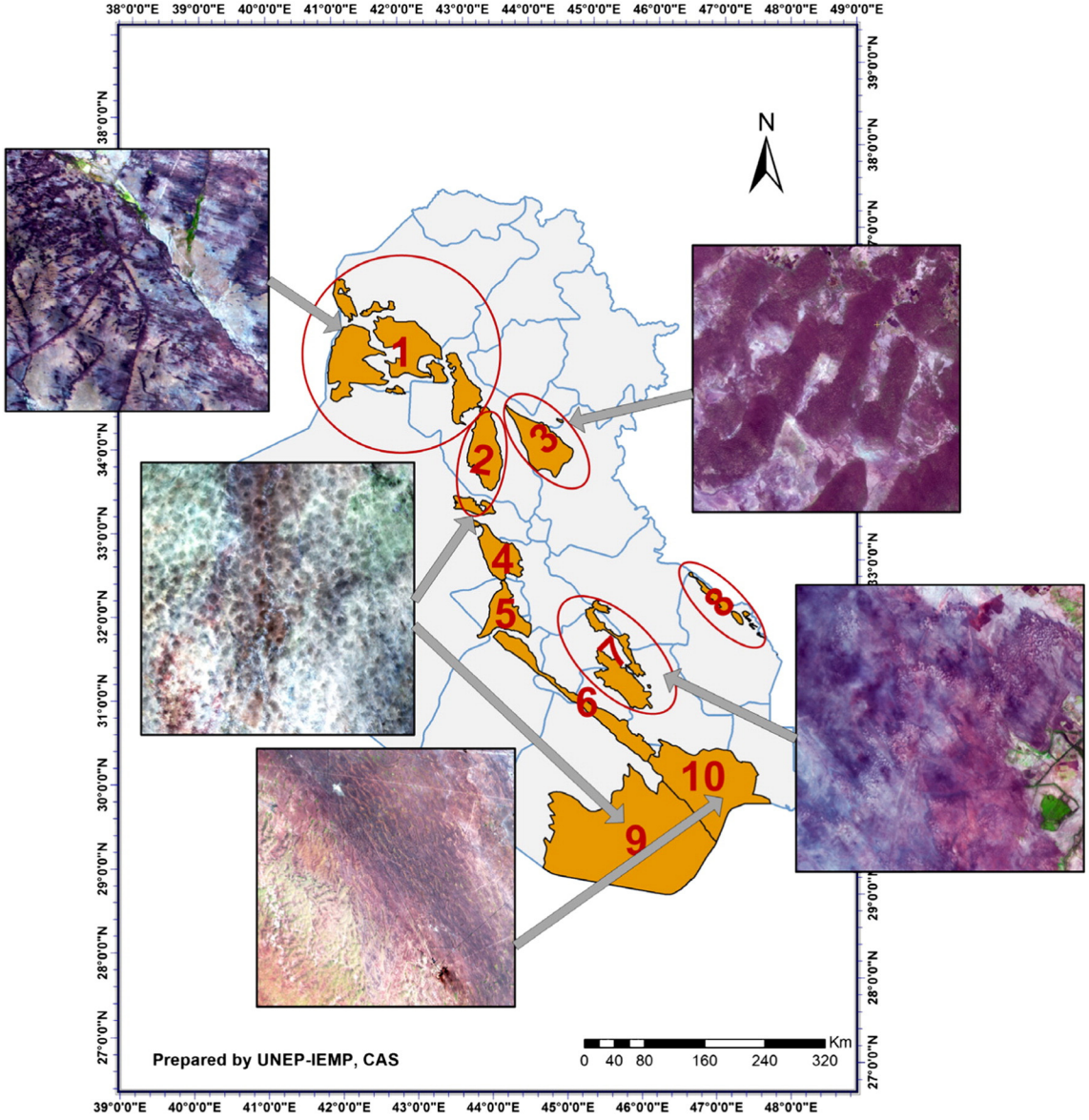

Fig. 7. Iraq SDS source area distribution and their characters on Landsat 8 images (6, 5, 4 bands). Ten source areas of different features are mapped out using visual interpretation combined with historical studies.

Table 2
Situation and features of SDS source areas in Iraq.

	Area (km^2)	Provinces	SDS (times)	Density (times/1000 km^2)
Area 1	12,514	Nineveh, Saladin	12	0.959
Area 2	4025	Saladin, Al-Anbar	11	2.733
Area 3	3524	Al-Anbar, Diyala	3	0.851
Area 4	2468	Al-Anbar, Babil	10	4.051
Area 5	2326	Karbala, Najaf	4	1.720
Area 6	3701	Najaf, Al-Qadisiyah, Muthannia	3	0.811
Area 7	3736	Al-Qadisiyah, Muthannia, Dhi-Qar	6	1.606
Area 8	826	Maysan	1	1.211
Area 9	24,760	Muthannia	4	0.162
Area 10	10,202	Muthannia, Dhi-Qar, Basra	4	0.392

amounts of oil wells are located in Area 2 and Area 4. Years of over-exploitation combined with frequent wind erosion has led to fast land degradation. Area 9 belongs to Zubair desert in Low Mesopotamia and is covered by calcareous deposits (Alonso-Pérez et al., 2013). The type of sand dunes in Area 5 and Area 10 is longitudinal dunes. Their formation is a result of wind trend which varies between at least two main directions. Area 10 including Mesopotamia marshes of southern Iraq has been degenerated rapidly since 2000 when they were subjected to ditching diking and draining (Richardson and Hussain, 2006). Areas 3, 6, 7, and 8 are early formed sand dunes in Iraq. Area 3 consists of transverse dunes and is exposed to the same wind most of the time (Kok et al., 2012), while sand dunes in Areas 6, 7, and 8 are barchans or barchans chains. Area 6 and Area 7 are regarded as strong aeolian SDS source areas and Area 8 is situated at the border of Iraq and Iran which is one of the SDS source areas mainly owing to frequent warfare in the past decades (Richardson and Hussain, 2006). Areas 3, 5, and 9, which are used to be alluvial fans, have been developed into SDS source regions after years of land degradation.

For the SDS events incorporated in this study, 18 dust storms happened or passed through Iraq. These dust events usually originate from Syria or Iraq territory, extending into different directions including Kuwait and Saudi Arabia, Persian Gulf or sometimes Iran (Sissakian et al., 2013). Table 2 shows the area, distribution, times and density of the SDS source areas. "Density" is represented as the ratio of "Times" and "Area".

$$Density = Times/Area \quad (3)$$

The higher the value, the more likely is this area to be considered as severe SDS source area. Based on Table 2, Areas 2, 4, 5, and 7 which have high "Density" values (more than 1.5) might be strong SDS source in Iraq. Areas 2, 4, and 5 are located on the way of two main SDS paths. One rises from the eastern part of Syria, passing through border of Iran and Syria, and extends deeply into Iraq, Iran or Saudi Arabia. The other path originates from north of Africa, always carrying massive sands and dusts and blowing over Jordan, south of Syria and northwest of Saudi Arabia. Area 7 is located on the way of a branch of Syria path and another path from central Asia dominating in dry season.

In addition to Syria, Iraq has become main dust source in West Asia affecting the western part of Iran, eastern Saudi Arabia, Kuwait and other Arabian countries. It is believed that within the next ten years, it would witness 300 dust storm events per year (JAPU, 2013).

3.1.3. SDS sources in Jordan, Iran and Saudi Arabia

The scenario to identify sand and dust storm source in Iran, Jordan and Saudi Arabia is slightly different from Syria and Iraq. We combined thematic maps with HYSPLIT mode results firstly. However, considering the scarce data and information available for these pilot countries, the major work will be accomplished using the interpretation experience of Syria and Iraq.

Jordan is divided into four main bioclimatic zones (Mediterranean region, Irano-Turanian region, Saharo-Arabian region and Sudanian Penetration) (Al-Bakri and Suleiman, 2004) in accordance with vegetation distribution and land cover/use. Besides the clues from land use/cover map, some vegetation types (Albert et al., 2004) such as sand dunes vegetation, weathered sandstone and granite scrub and sandy Hammada which lie in desert or semi-desert regions are recognized as potential SDS sources. Generally, there are two main SDS source regions (Fig. 8(a)) consistent with the scope of "sand plain" in Jordan's land cover/use map (Al-Bakri et al., 2013). The western part of Area 2 is covered by star dunes and formed by sand deposition on mountainous area. So, it may not be a severe SDS source region because of the terrain limitation. Area 1 and the Eastern part of Area 2 are subjected to relatively strong aeolian erosion and sand transportation which is confirmed by the existence of long sand stripes. Both SDS source areas are under control of prevailing wind from Mediterranean Sea or coastal of north of Africa (Abed et al., 2009), but they occupy different paths into the inland. Sands from Area 1 are often blown to Iraq while Area 2 mainly affects northern and central Saudi Arabia.

Iran consists of four SDS source regions (Fig. 8(b)), of which, Areas 1 and 2 lie in Al-Howizeh/Al-Azim marshes (Gerivani et al., 2011), Area 3 lies within Sistan Plain and Area 4 lies in the coastal region of Oman Gulf. Area 1 is covered by fine sand dunes which are regarded as the extension of the SDS source areas in Iraq border (Fig. 7, Area 8). Area 2 is suffering from fast land degradation owing to the drying out of Horol Azim Lake, the damage of more than 15 million palm trees during the war (which could resist wind erosion) (Morabbi, 2011). Situated in the dust storm path which passes Iraq border SDS source, Area 2 also experiences huge sand deposition. The land degradation in Area 3 is growing severely. Furthermore, this region suffers from much stronger aeolian sediments due to dust storms which are originated above Area 3 and hit Sistan and Baluchestan province in Iran and southern Afghanistan (Ekhtesasi and Gohari, 2013). Although Area 4 is relatively small, dust storms that happened here will present vast economic damages to the southern Iranian coast (Wilderson, 1991).

Saudi Arabia is dominated by Arabian Desert (Rizvi, 1989). In the scenario for Saudi Arabia SDS source generation, deserts were mapped out firstly. SDS source (Fig. 8(c)) is recognized after analyzing sand texture (sand distribution trend and strip direction) and dominant dust storms path (prevailing wind). Saudi Arabia SDS source also comprises four main regions. Areas 1, 2 and 4 are under the control of depression from southeast Mediterranean Sea and north of Africa. However, these three SDS source regions have different dust storm paths. Sands raised from Area 1, accompanied with the source in southeast of Jordan, mainly affect north and center of Saudi Arabia (Wilderson, 1991). The character of Area 2 is consistent with SDS source in northeast of Jordan. Dust storms from Sudan in north of Africa always pass over Red Sea and south of Saudi Arabia, hitting Kuwait and central Iraq through Area 3 or Iran through Area 4 (Banks and Brindley, 2013; Hamidi et al., 2014).

3.2. SDS clusters and paths in West Asia

The climate in West Asia is divided into four main systems: the Siberian anticyclone in winter over central Asia; the Polar anticyclone

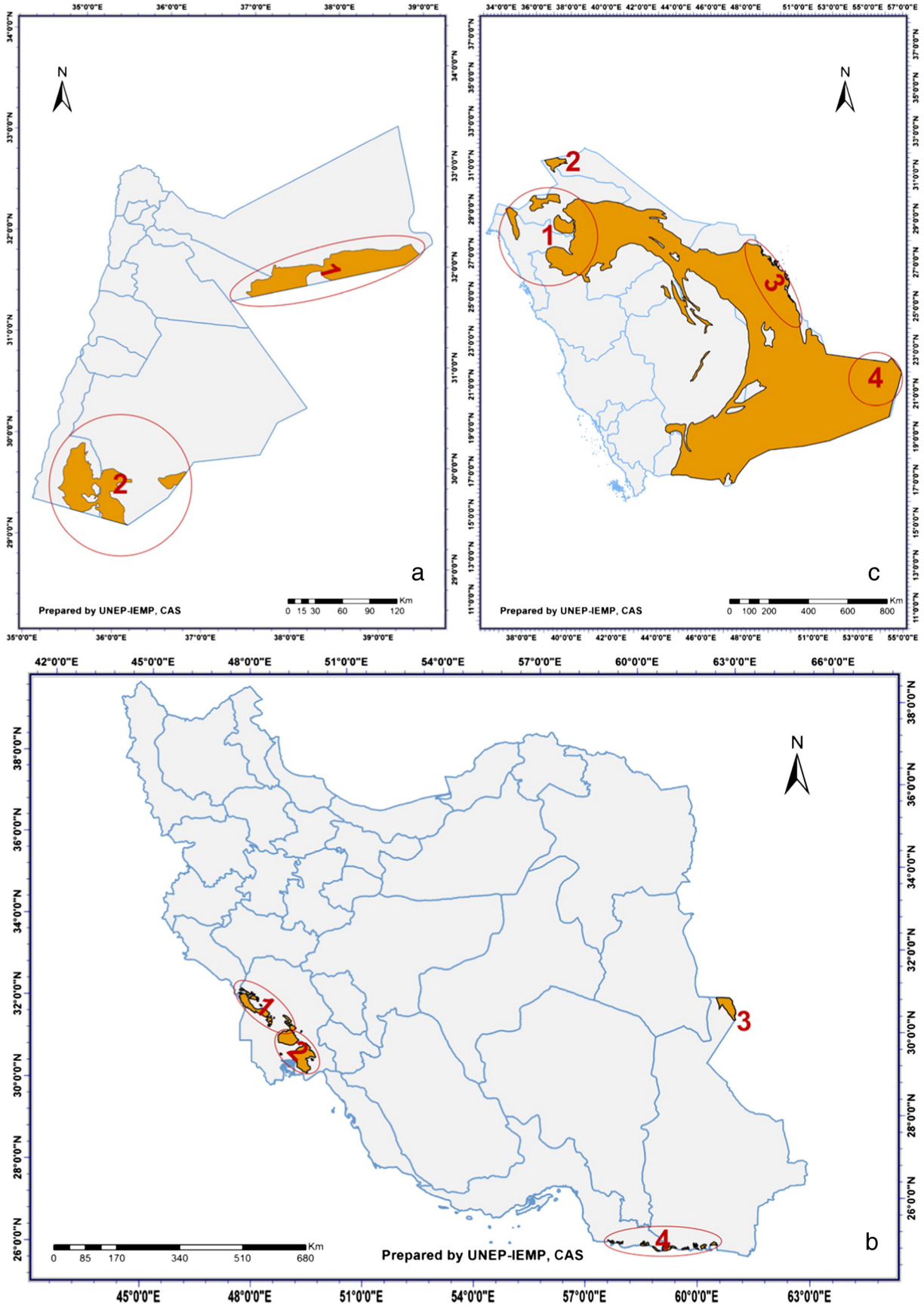

Fig. 8. SDS source areas distribution in Jordan, Iran and Saudi Arabia.

in summer over east of Europe and Mediterranean Sea; the monsoon cyclones in summer over the India Subcontinent, south and southeast of Iran and southeast of Arabian peninsula; the depressions traveling from north of Africa and south and east of Mediterranean sea across the Middle East and southwest of Asia in the non-summer seasons (Hamidi et al., 2013). These climate systems have shown strong effects on the distribution of SDS.

In West Asia, most of dust storm systems can be classified into Summer Shamal and Frontal dust storms (Hamidi et al., 2013). Shamal dust storm usually occurs across Iraq, Kuwait, western part of Khuzestan plain and some parts of Arabian Peninsula (Middleton, 1986). Summer shamal is basically generated by a zone of convergence between the subtropical ridge, extending into the northern Arabian Peninsula and Iraq from the Mediterranean Sea and Monsoon Trough across southern Iran and southern Arabian Peninsula (Hamidi et al., 2013). Frontal dust storms are dynamic synoptic systems that mix the dust in the air and carry it for greater distances in non-summer seasons. There are three types of frontal dust storms: prefrontal, postfrontal and shear-line. Prefrontal dust storms occur across Jordan, Israel, the northern Arabian Peninsula, Iraq and western Khuzestan Plains of Iran, as low-pressure area move across the region (Wilderson, 1991). Postfrontal dust storms are referred as a winter Shamal across most of Middle East. Shear-lines are the result of the convergence of north-easterly wind flow to the south of a polar high-pressure cell and the easterly trade-wind flow (Middleton, 1986).

Finally, SDS source clusters and main paths (Fig. 9) are generated according to the features of SDS source areas on images, climate and geography, and knowledge from historical studies. There are 6 main SDS paths dominated by the climate in West Asia.

(1) The first path originates from Mediterranean Sea passing over Cyprus and enters into Syria. It turns to southeast through the Syria–Iraq border and extends into central Iraq. Commonly, this path will go further to south of Iraq, Kuwait and Persian Gulf. While crossing with other streams, it usually has alternative destinations. One moves toward south Iraq and Saudi Arabia through southern border of Iraq and Saudi Arabia. The other one turns right, across Iraq–Iran border and terminates in Iran (Sissakian et al., 2013).

(2) The second path is under the control of high pressure system over east of Europe (Hamidi et al., 2013). This path gets similar situation with the first one, which has two common branches. When arriving central Iraq through the northern border, it either hits Iran through the Iraq–Iran border or east of Saudi Arabia through south of Iraq border and Kuwait.

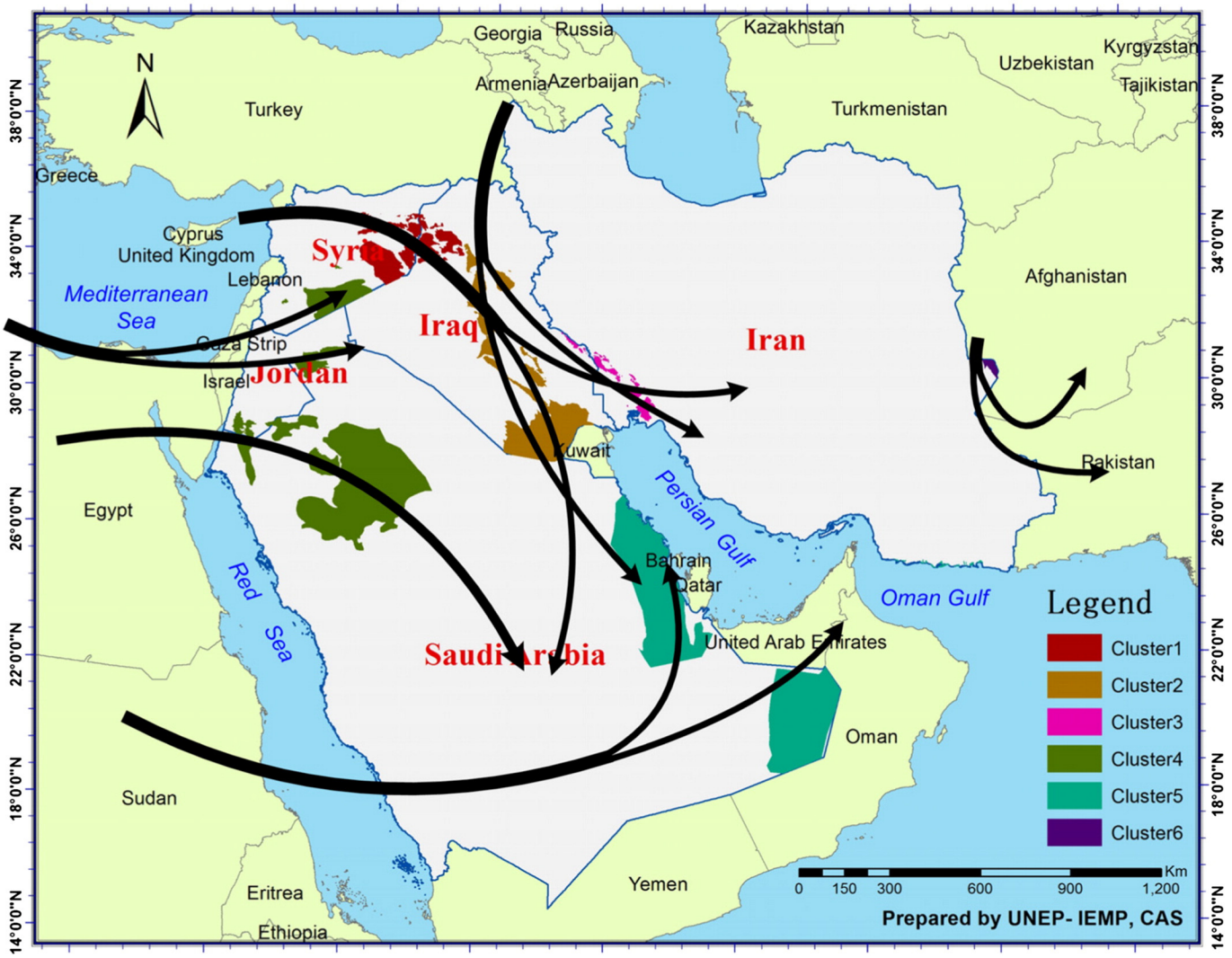

Fig. 9. SDS main paths and source clusters in West Asia.

(3) The third path comes from south of Mediterranean Sea or coastal of northern Africa and always strikes south of Syria or north border of Jordan and Saudi Arabia (Wilderson, 1991).
(4) The fourth path is from north of Africa which usually passes across Egypt, north of Red Sea and blows toward southeast in Saudi Arabia.
(5) The fifth path is also located in the depressions in north of Africa. However, it usually passes south of Saudi Arabia through Sudan or Red Sea (Hamidi et al., 2014). Sometimes this path will turn upward to east of Saudi Arabia or even Iran across Persian Gulf if encountering the monsoon cyclones from Indian Subcontinent. Otherwise, it might extend into southeast of Arabian Peninsula or Iran by Oman Gulf (Banks and Brindley, 2013).
(6) The last path originates from Sistan Plain at the Iran–Afghanistan border which is controlled by anticyclone over central Asia. It mainly hits Sistan and Baluchistan Province in Iran and then moves forward to Pakistan or makes a U-turn to Afghanistan (Rezazadeh et al., 2013).

Besides these main paths, there are occasional convergences of different paths (paths from Mediterranean Sea, east of Europe, Indian subcontinent in summer or from central Asia and north of Africa in spring and winter), which may sometimes lead to super dust storms. The first two paths are highly associated with Summer Shamal dust storms. Paths (3) and (4) have shown similar trajectories with Prefrontal dust storms while path (5) is related with Shear-line dust storms.

With the homogeneity of features (wind erosion stripes, color and continuity, etc.), origin and trajectory of air masses and the classification of historical studies, SDS clusters can be identified accordingly. In Fig. 9, Cluster 1, including northeast of Syria and Syria-Iraq border, lies on the way of the first path from Mediterranean Sea. These two parts have shown homogeneity of textures on the satellite images and continuity in the geography. Cluster 3, which has been identified by the same reason based on homogeneity and continuity, is situated in Iraq-Iran border (Gerivani et al., 2011; UNEP, 2013). Cluster 2 consists of the rest source areas in Iraq. Based on observations of wind erosion events on Landsat 8 images, central Iraq was considered as the most severe source area in this Cluster. Both Clusters 2 and 3 are affected in the convergence of the paths from Mediterranean Sea (first path) and east of Europe (second path). Located in the right side of the Tigris–Euphrates alluvial plain, Clusters 1–3 are considered as main sources for Iran (Zoljoodi et al., 2013), Saudi Arabia and some other Arabian countries. Cluster 4 includes three regions, the source area in south of Syria, border of Jordan and Saudi Arabia, and the source area in northwest of Saudi Arabia. Actually, areas in the south Syria and northern border of Jordan-Saudi Arabia, both situated in Syrian Desert, are much more correlated to each other. Areas in the northwest Saudi Arabia and south border of Jordan-Saudi Arabia present a higher homogeneity. Nevertheless, these areas are clustered given that all of them are affected by air masses from south coast of Mediterranean Sea or north of Africa and regarded as red sea source area (Wilderson, 1991). Cluster 5 is mapped out generally (actually no precise scope considering the large amounts of sand dunes in Saudi Arabia). It is on the way of the fifth path and considered as the dust source of Iran coastal areas (Hamidi et al., 2014; Washington et al., 2003). Cluster 6, as one of the two prominent SDS source clusters in Iran (Gerivani et al., 2011), locates in north of Sistan and Baluchistan province and affects Pakistan and Afghanistan (Rashki et al., 2012). These clusters correspond well to the SDS frequency map in Fig. 2 and consist of the main SDS source in West Asia.

4. Conclusions

In this paper, thematic maps based on previous studies were firstly employed as clues for SDS source areas in West Asia. In the second step, SDS source points were extracted combining thematic maps and HYSPLIT simulated trajectories. HYSPLIT Model is only suitable for the simulation of single trajectory. Thus, only 27 simulated trajectories of dust events were consistent with the real situation showing in MODIS images. After summarizing the features of SDS points, the whole SDS sources in West Asia were interpreted on Landsat 8 images based on existing research, climate and geography, and SDS trajectories on MODIS images.

The result presented shows specific SDS source distributions in the pilot countries. According to Fig. 9 and the MODIS L1B images (a collection of more than 50 dust storm events), the Tigris–Euphrates alluvial plain, which includes SDS source in eastern Syria, Iraq and the Iran–Iraq border, is recognized as the main dust source in West Asia. Although Saudi Arabia is covered by large quantity of fine sands, it may not be a severe SDS source at regional scale. Air masses from Mediterranean Sea are important factors for the generation of sand and dust storms which cover about 70% dust storm events in our research. The depression in North Africa mainly affects south of Syria, Jordan and western Saudi Arabia while the monsoon cyclones from Indian subcontinent always hits south of Iran and southeast of Arabian Peninsula. Dust storms that happened in Clusters 1–4 (Fig. 7) are mainly part of shamal or prefrontal dust storms in summer, and postfrontal dust storms in winter. Shear-lines always occur over north of Africa, Red Sea, west of Arabian Peninsula and sweep over Cluster 5.

This paper as an initiative effort generated the integrated SDS source areas at a regional scale in West Asia (Syria, Iraq, Iran, Jordan, Saudi Arabia), with precise geographic position and scope. Having knowledge on the exact SDS source areas and paths, we can ascertain the dust generation and transportation in West Asia. Besides, focusing on SDS source areas is also a key process in combating sand and dust storms.

Acknowledgment

This research is funded by the Small Scale Funding Agreement (UNEP/ROWA). The first author appreciates Dr Yongdong Wang from Xinjiang Institute of Ecology and Geography, Chinese Academy of Sciences for the great and valuable help in data collection. Farshad Amiraslani acknowledges the University of Tehran for providing a six-month Research Leave Grant (#171/122133; 1392/6/4). His research was also supported by the Chinese Academy of Sciences Visiting Fellowship for Researchers from Developing Countries (Grant # 2013FFZA0013) during the visiting period at UNEP-IEMP. The authors are also grateful to NOAA Air Resources Laboratory (ARL) for the support of HYSPLIT online model.

References

Abed AM, Al Kuisi M, Khair HA. Characterization of the Khamaseen (spring) dust in Jordan. Atmos Environ 2009;43:2868–76.
Al-Bakri JT, Suleiman AS. NDVI response to rainfall in different ecological zones in Jordan. Int J Remote Sens 2004;25:3897–912.
Al-Bakri J, Salahat M, Suleiman A, Suifan M, Hamdan M, Khresat S, et al. Impact of climate and land Use changes on water and food security in Jordan: implications for transcending "the tragedy of the commons". Sustainability 2013;5:724–48.
Albert R, Bibiane B, Watzka M. Zur Vegetation und Flora Jordaniens. Reise Durch Die Natur Jordaniens. Denesia 2004;14:133–220.
Al-Hurban AE, Al-Ostad AN. Textural characteristics of dust fallout and potential effect on public health in Kuwait City and suburbs. Environ Earth Sci 2009;60:169–81.
Al-Jumaily KJ, Ibrahim MK. Analysis of synoptic situation for dust storms in Iraq. Int J Energy Environ 2013;4:851–8.
Almasi A, Mousavi AR, Bakhshi S, Namdari F. Dust storms and environmental health impacts; 2014. p. 353–6.
Alonso-Pérez S, Al-Dabbas M, Mohammed AAA, Al-Waeli THH. Establishing a national programme to combat sand and dust storms in Iraq; 2013.
Amiraslani F, Dragovich D. Combating desertification in Iran over the last 50 years: an overview of changing approaches. J Environ Manage 2011;92:1–13.
Ashrafi Khosro, Shafiepour-Motlagh Majid, Aslemand Alireza, Ghader S. Dust storm simulation over Iran using HYSPLIT. J Environ Health Sci Eng 2014;12:9.
Banks JR, Brindley HE. Evaluation of MSG-SEVIRI mineral dust retrieval products over North Africa and the Middle East. Remote Sens Environ 2013;128:58–73.
Barnum B, Winstead N, Wesely J, Hakola A, Colarco P, Toon O, et al. Forecasting dust storms using the CARMA-dust model and MM5 weather data. Environ Model Software 2004;19:129–40.

Boloorani AD, Nabavi S, Azizi R, Bahrami H. Characterization of dust storm sources in western Iran using a synthetic approach. 415–420. Advances in meteorology, climatology and atmospheric physicsSpringer; 2013.
Bsoul Eng Majed, Mazahreh ES. Available information about soil, current land cover/land use in Jordan. Inception workshop on Regional Soil Partnership and MENA Soil Information System; 2012.
Draxler RR, Hess GD. Description of the HYSPLIT_4 modeling system. Air Resources Laboratory; 1997.
Draxler RR, Hess GD. An overview of the HYSPLIT_4 modelling system for trajectories, dispersion, and deposition. Aust Meteorol Mag 1998;47:395-308.
Draxler RR, Gillette DA, Kirkpatrick JS, Heller J. Estimating PM^{10} air concentrations from dust storms in Iraq, Kuwait and Saudi Arabia. Atmos Environ 2001;35:4315–30.
DRI. Integrated desert terrain forecasting for military operations (DTF). Desert Research Institute; 2012.
Ekhtesasi M, Gohari Z. Determining area affected by dust storms in different wind speeds, using satellite images (case study: SISTAN PLAIN, IRAN). Desert 2013;17. 193-202.
Esmaili O, Tajrishy M, Arasteh PD. Evaluation of dust sources in Iran through remote sensing and synoptical analysis. Atlantic Europe conference on remote imaging and, spectroscopy; 2006a. p. 136–43.
Esmaili O, Tajrishy M, Arasteh PD. Results of the 50 year ground-based measurements in comparison with satellite remote sensing of two prominent dust emission sources located in Iran. Remote sensing of clouds and the atmosphere XI. International Society for Optics and Photonics; 2006b. p. 636209–12.
Furman HKH. Dust storms in the Middle East: sources of origin and their temporal characteristics. Indoor Built Environ 2003;12:419–26.
Geerken R, Ilaiwi M. Assessment of rangeland degradation and development of a strategy for rehabilitation. Remote Sens Environ 2004;90:490–504.
Gerivani H, Lashkaripour GR, Ghafoori M. The source of dust storm in Iran: a case study based on geological information and rainfall data. Carpath J Earth Environ Sci 2011; 6:297–308.
Ginoux P, Chin M, Tegen I, Prospero JM, Holben B, Dubovik O, et al. Sources and distributions of dust aerosols simulated with the GOCART model. J Geophys Res 2001;106: 20255–73.
Goudie AS. Dust storms: recent developments. J Environ Manage 2009;90:89–94.
Hamidi M, Kavianpour MR, Shao Y. Synoptic analysis of dust storms in the Middle East. Asia-Pac J Atmos Sci 2013;49:279–86.
Hamidi M, Kavianpour MR, Shao Y. Numerical simulation of dust events in the Middle East. Aeolian Res 2014;13:59–70.
Hereher ME. Sand movement patterns in the Western Desert of Egypt: an environmental concern. Environ Earth Sci 2009;59:1119–27.
IFAD. Syrian Arab Republic: thematic study on land reclamation through de-rocking. Near East and North Africa Division; 2007.
Ilaiwi M. Soils of the Syrian Arab Republic. Soil resources of Southern and Eastern Mediterranean countries. Bari: Centre international de hautes études agronomiques méditerranéennes-Instituto Agronomico Mediterraneo di Bari (Ciheam-IAMB); 2001.
JAPU. Sand and dust storms fact sheet. Unit(JAPU) JAaP. UN; 2013.
Keramat A, Marivani B, Samsami M. Climatic change, drought and dust crisis in Iran. WASET 2011;6:10–3.
Kok JF, Parteli EJ, Michaels TI, Karam DB. The physics of wind-blown sand and dust. Rep Prog Phys 2012;75:106901.
Li P, Jiang L, Feng Z. Cross-comparison of vegetation indices derived from Landsat-7 enhanced thematic mapper plus (ETM+) and Landsat-8 operational land imager (OLI) sensors. Remote Sens. 2013;6:310–29.
Liu M, Westphal DL, Walker AL, Holt TR, Richardson KA, Miller SD. COAMPS real-time dust storm forecasting during operation Iraqi freedom. Weather Forecast 2007;22: 192–206.
Lu H, Shao Y. Toward quantitative prediction of dust storms: an integrated wind erosion modelling system and its applications. Environ Model Software 2001;16:233–49.
Menéndez I, Diaz-Hernandez J, Mangas J, Alonso I, Sanchez-Soto P. Airborne dust accumulation and soil development in the North-East sector of Gran Canaria (Canary Islands, Spain). J Arid Environ 2007;71:57–81.
Middleton N. Dust storms in the Middle East. J Arid Environ 1986;10:83–96.
Mohammad R. Using thermal infrared (TIR) data to characterize dust storms and their sources in the Middle East. University of Pittsburgh; 2012.
Morabbi M. Risk warning and crisis management for dust storm effects on western border of Iran. United Nations international conference on space-based technologies for disaster risk management United Nations; 2011.
PME. First national communication Kingdom of Saudi Arabia. Presidency of Meteorology and Environment (PME); 2005.
Prospero JM. Environmental characterization of global sources of atmospheric soil dust identified with the NIMBUS 7 Total Ozone Mapping Spectrometer (TOMS) absorbing aerosol product. Rev Geophys 2002;40.
Rashki A, Kaskaoutis DG, CJd Rautenbach, Eriksson PG, Qiang M, Gupta P. Dust storms and their horizontal dust loading in the Sistan region, Iran. Aeolian Res 2012;5:51–62.
Rezazadeh M, Irannejad P, Shao Y. Climatology of the Middle East dust events. Aeolian Res 2013;10:103–9.
Richardson CJ, Hussain NA. Restoring the Garden of Eden: an ecological assessment of the marshes of Iraq. BioScience 2006;56:477–89.
Rizvi AA. Planning responses to Aeolian hazards in arid regions. J King Saud Univ 1989;1: 59–74.
Sissakian VK, Al-Ansari N, Knutsson S. Sand and dust storm events in Iraq. Nat Sci 2013; 05:1084–94.
Small I, Van der Meer J, Upshur R. Acting on an environmental health disaster: the case of the Aral Sea. Environ Health Perspect 2001;109:547.
Taheri Shahraiyni H, Karimi K, Habibi Nokhandan M, Hafezi Moghadas N. Monitoring of dust storm and estimation of aerosol concentration in the Middle East using remotely sensed images. Arab J Geosci 2014;10.
Tsolmon R, Ochirkhuyag L, Sternberg T. Monitoring the source of trans-national dust storms in north East Asia. Int J Digit Earth 2008;1:119–29.
UNDP. National action plan to combat desertification in the Syria Arab Republic. In: UNDP, editor. Directorate MoSfEAL; 2002.
UNEP. UNEP pilot project: dust storm hot spots in Islamic Republic of Iran. Geoinformatics Research Institute (GRI); 2013.
Wang Y, Stein AF, Draxler RR, de la Rosa JD, Zhang X. Global sand and dust storms in 2008: observation and HYSPLIT model verification. Atmos Environ 2011;45:6368–81.
Washington R, Todd M, Middleton NJ, Goudie AS. Dust-storm source areas determined by the total ozone monitoring spectrometer and surface observations. Ann Assoc Am Geogr 2003;93:297–313.
Wilderson WD. Dust and sand forecasting in Iraq and adjoining countries. DTIC document; 1991.
Wmo U. Establishing a WMO sand and dust storm warning advisory and assessment system regional node for West Asia: current capabilities and needs; 2013.
Wong S, Dessler AE. Suppression of deep convection over the tropical North Atlantic by the Saharan Air Layer. Geophys Res Lett 2005;32.
Yang Y, Squires V, Lu Q. Global alarm: dust and sandstorms from the world's drylands. United Nations Convention to Combat Desertification, Bangkok; 2001. p. 345.
Zhang B, Tsunekawa A, Tsubo M. Contributions of sandy lands and stony deserts to long-distance dust emission in China and Mongolia during 2000–2006. Global Planet Change 2008;60:487–504.
Zoljoodi M, Didevarasl A, Saadatabadi AR. Dust events in the western parts of Iran and the relationship with drought expansion over the dust-source areas in Iraq and Syria. Atmos Clim Sci 2013;03:321–36.